



Functional substrate analysis in patients with persistent atrial fibrillation

Pietro Rossi¹ · Michele Magnocavallo¹ · Filippo Maria Cauti² · Marco PolSELLI¹ · Marta NISCOLA³ · Domenico Giovanni Della Rocca⁴ · Ambra del Greco³ · Luigi Iaia¹ · Raffaele Quaglione⁵ · Piccirillo Gianfranco⁵ · Stefano Bianchi¹

Received: 28 February 2024 / Accepted: 29 April 2024

© The Author(s), under exclusive licence to Springer Science+Business Media, LLC, part of Springer Nature 2024

Abstract

Objectives The aim of this study was to describe the correlation between atrial electrogram duration map (AEDUM), spatiotemporal electrogram dispersion (STED) and low voltage areas (LVA) in patients with persistent atrial fibrillation (*PsAF*).

Background The degree of left atrial (LA) tissue remodelling and augmented anisotropic conduction is one of the major issues related to *PsAF* ablation outcome.

Methods This study enrolled consecutive patients with *PsAF* undergoing pulmonary vein isolation. In all patients, voltage, AEDUM and STED maps were created, and the correlation was reported between these three mapping methods.

Results A total of 40 patients with *PsAF* were enrolled. The mean age was 62.2 ± 7.4 years, and males were 72.5% ($n = 29$). The overall bipolar voltage of the LA was 3.06 ± 1.87 mV. All patients had at least one AEDUM area (overall AEDUM area: 21.8 ± 8.2 cm²); the mean longest electrogram (EGMs) duration was 90 ± 19 ms. STED areas with < 120 ms was 46.3 ± 20.2 cm² which covered $45 \pm 22\%$ of the LA surface. AEDUM and STED areas were most frequently reported on the roof, the anterior wall and the septum. The extension of the AEDUM areas was significantly smaller than STED areas with CL < 120 ms (21.8 ± 8.2 vs 46.3 ± 20.2 ; p -value < 0.0001). In 24 patients (60%), AEDUM areas were entirely included in the STED areas with CL < 120 ms. In the three (7.5%) patients with LVA, no correspondence with STED and AEDUM was noted.

Conclusion AEDUM and STED maps allow to identify areas of conductive dysfunction as a possible atrial substrate even if a normal voltage is detected.

Pietro Rossi and Michele Magnocavallo contributed equally to this work.

✉ Pietro Rossi
ptr.rossi@gmail.com

¹ Arrhythmology Unit, Isola Tiberina – Gemelli Isola, Rome, Italy

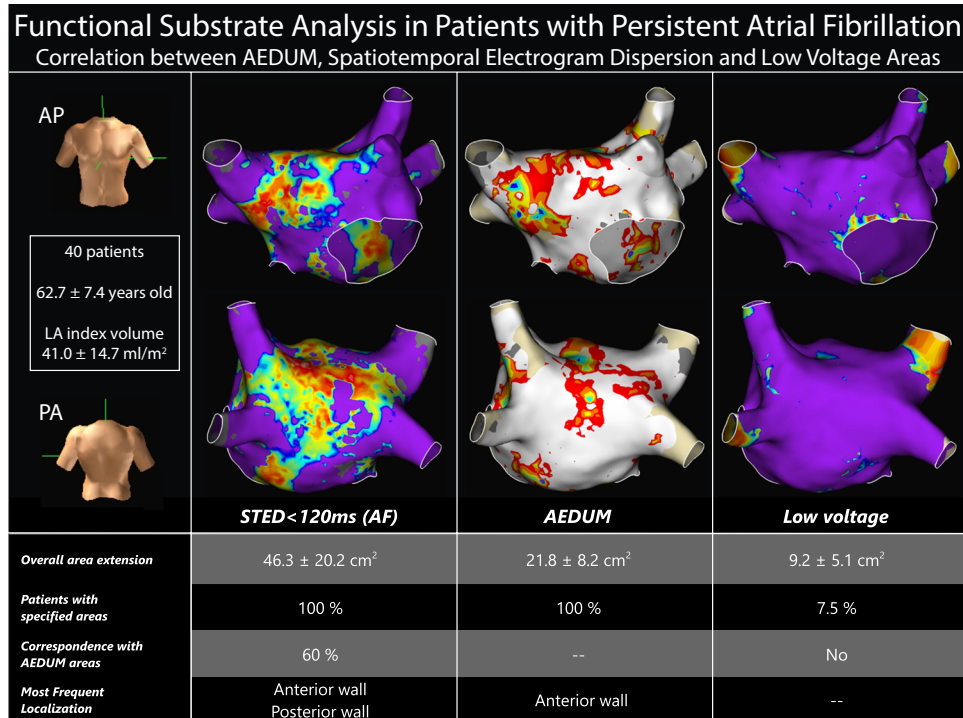
² Arrhythmology Department, IRCCS San Raffaele Scientific Institute, Milan, Italy

³ Abbott Medical, Via Paracelso 20, 20864 Agrate Brianza, Italy

⁴ Heart Rhythm Management Centre, Postgraduate Program in Cardiac Electrophysiology and Pacing, European Reference Networks Guard – Heart, Universitair Ziekenhuis Brussel-Vrije Universiteit Brussel, Brussels, Belgium

⁵ Department of Internal, Anesthesiology and Cardiovascular Sciences, Policlinico Umberto I, Sapienza University of Rome, 00185 Rome, Italy

Graphical Abstract



Keywords Persistent atrial fibrillation · Complex fractionated atrial electrograms · Spatiotemporal electrogram dispersion · Electrogram duration · AEDUM · Low voltage · Functional substrate

Abbreviations

AEDUM	Atrial electrogram duration map
AF	Atrial fibrillation
CFAE	Complex fractionated atrial electrograms
CL	Cycle length
ECV	Electrical cardioversion
EGM	Electrogram
LA	Left atria
LVA	Low voltage area
<i>P</i> sAF	Persistent atrial fibrillation
PVI	Pulmonary vein isolation
SR	Sinus rhythm
STED	Spatiotemporal electrogram dispersion

1 Introduction

Pulmonary vein isolation (PVI) is the cornerstone of interventional management of atrial fibrillation (AF) [1]. PVI is also considered an appropriate therapeutic strategy for persistent AF (*P*sAF) but is less effective [2, 3]. Major issues pertaining to *P*sAF recurrence depend on the extent, localization and the degree of atrial tissue damages [4].

Atrial tissue remodelling is characterized by patchy and interstitial fibrosis and by changes in spatial distribution of intercellular connexins. These alterations cause disturbances in wave propagation between cardiomyocytes thus contributing to non-uniform anisotropic conduction, which may eventually create the substrate for re-entry and maintenance of arrhythmias [5–8]. Many approaches have been proposed to detect and measure left atrial (LA) tissue dysfunctional areas: the identification of low voltage zone during AF [9–11], the evaluation of complex fractionated atrial electrograms (CFAE) [12], the mapping of the functional rotational activity maintaining AF [13] as well as areas of spatiotemporal electrogram dispersion (STED) [14]. Among them, STED seems to be the most promising approach for the identification and subsequently ablation of fibrosis areas [15, 16].

A novel functional substrate electroanatomical map — atrial electrogram duration map (AEDUM) — based on the local duration of the bipolar electrogram (EGM) registered in sinus rhythm (SR) was recently developed [17]. The AEDUM approach is founded on the assumption that prolonged EGMs (≥ 45 ms) identify areas of slow and inhomogeneous activation potentially critical for the

maintaining of AF. Although the AEDUM approach was tested in a small cohort of patients, the ablation approach targeting the AEDUM areas seems to be a feasible and effective strategy to treat patients with PsAF [17].

The aim of this study is to evaluate the correlation between AEDUM, spatiotemporal electrogram dispersion and low voltage areas (LVA) in patients with PsAF.

2 Methods

2.1 Study population

Patients who met the standard indications for PsAF ablation were retrospectively enrolled in this study from May 2019 [1]. All procedures were performed at the Arrhythmology Unit of the Isola Tiberina – Gemelli Isola Hospital, Rome, Italy. Exclusion criteria were uncontrolled hypertension, severe valvular dysfunctions, uncontrolled thyroid disease, severe chronic obstructive pulmonary disease, alcohol/drug abuse and systemic inflammatory diseases. Anti-arrhythmic medications were discontinued at least 5 half-lives before hospital admission. Amiodarone administration was interrupted at least 1 month before ablation. The study protocol was approved by the local ethics committee, and written informed consent from all patients was obtained before each procedure.

2.2 Mapping procedure

All procedures were conducted under general anaesthesia. After mapping during AF, electrical cardioversion (ECV) was performed, and a SR map was then obtained. A second ECV was performed after PVI in the case SR was not restored or AF was triggered again during mapping. All procedures were performed using the EnSite Precision™ Mapping System and the multipolar diagnostic catheter Advisor™ HD Grid Mapping Catheter, Sensor Enabled™ (Abbott, Minneapolis, MN, USA), using HD-wave configuration.

2.2.1 Voltage map

The voltage map was created by using the EnSite Precision AutoMap Mapping Tool™. Automatic mapping criteria were set as follows: score threshold 90%, speed limit 10 mm/s, distance 0.1 mm, signal-to-noise 5, and enhanced noise rejection on. LVA were defined as having bipolar voltage < 0.5 mV [18]. Bipolar EGMs were filtered at 30 and 300 Hz. The substrate map's interpolation, interior projection and exterior projection were all set to 7.

2.2.2 AEDUM map

EGM duration was measured through the Ensite Precision Automatic Turbomap Tool which allowed to review SR maps and calculate the duration of each point's EGM as the temporal distance (ms) between the first and last deflection of each bipolar endocardial EGM [17, 19].

An experienced biomedical engineer verified the measurement of the EGM duration intraoperatively after having completed the LA map. The points used to measure the EGM duration were carefully reviewed also offline to confirm the correct measurement. The AEDUM map shows through a color-coded representation the distribution of EGM durations. A cut-off value of 45 ms was chosen to identify areas of atrial conductive dysfunction, and zones with EGMs longer than 45 ms were defined as AEDUM areas.

2.2.3 STED map

STED maps during PsAF were performed through Ensite Precision CFAE Mapping Tool. As previously validated, the algorithm measures the time interval between multiple, discrete deflections in a local AF EGM recording over an 8-s data interval and then averages the inter-deflection time intervals to calculate the mean cycle length (CL) of the local EGM during AF [7, 20]. This means CL is then projected onto the LA anatomical shell as a colour-coded display, simultaneously applied for each recording HD Grid bipole. The shorter the CL, the more rapid and fractionated the local EGM. User-defined peak-to-peak EGM amplitude, EGM width and post-EGM refractory period were selected to assist in algorithm deflection detection and have been previously validated. Deflection width, sensitivity and refractory criteria were set at 20 ms, 0.05 mV and 50 ms, respectively, to avoid double-counting individual EGM deflections and taking into consideration a noise floor of 0.01 mV. Specifically for this study, areas displaying "STED" were characterized by a mean CL of less than either 60 or 120 ms and by colour crowding in the LA geometry (Fig. 1).

2.3 Analysis of AEDUM and STED areas

The LA was divided into 14 segments as previously reported [21]. The following were noted for each patient: (1) the extent of the total area with voltage < 0.5 mV during SR and the corresponding segments; (2) AEDUM areas and corresponding segments during; (3) STED areas and corresponding segments during AF with both CLs mean < 60 ms and between 60 and 120 ms; (4) the prolonged EGMs for each patient were independently analysed by two electrophysiologist (PR and MM) to identify slow and fast components of the signal. Fast components were defined as at

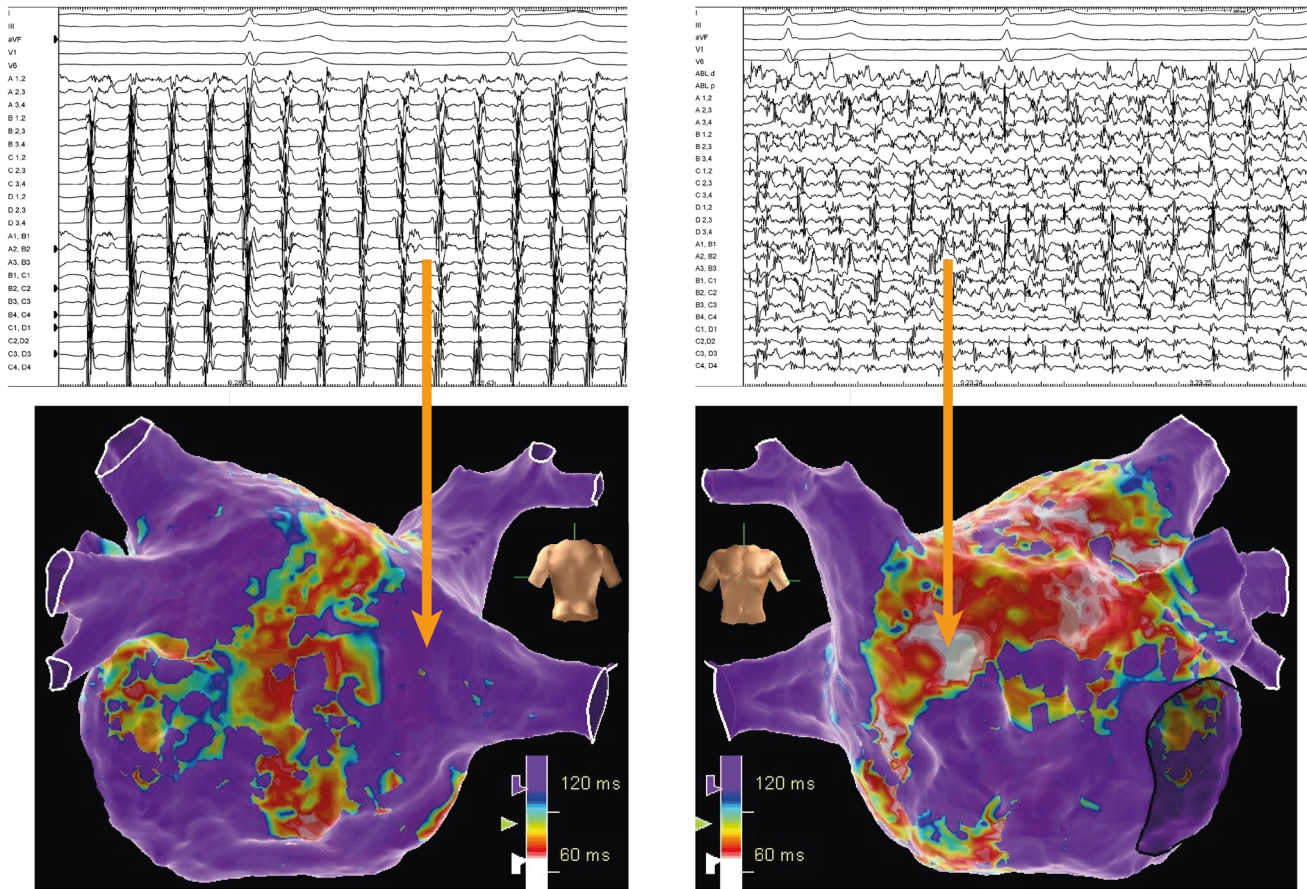


Fig. 1 STED map. Ensite Precision CFAE Mapping Tool reconstructs STED maps measuring mean time interval between multiple, discrete deflections in a local AF EGM recording. More fractionated and rapid local EGM correlate to shorter cycle length and are represented in a color-coded scale. This figure shows the posterior and anterior views of the LA STED map of a representative patient. The arrow in the left panel indicates a LA region in the posterior wall not exhibiting

STED (represented in violet which corresponds to a STED > 120 ms) in which the EGMs shown were obtained. The right panel shows the LA anterior view in which a high degree of STED has been found, and the EGMs shown were obtained from the LA region represented in white, corresponding to a STED < 60 ms. AF, atrial fibrillation; EGM, eElectrogram; LA, left atrium; STED, spatiotemporal electrogram dispersion

least two inversions in signal direction during 15 ms; (5) maximum AEDUM EGM duration and their standard deviations; (6) the degree of overlap among areas of AEDUM in SR and STED (CL < 120 ms) for each patient.

2.4 Statistical analysis

The normal distribution of all continuous variables was checked by visual methods (Q-Q plot and histogram) and by the significance test (Kolmogorov–Smirnov normality test and Shapiro–Wilk’s test). For continuous variables, descriptive statistics were provided (number of available observations, mean and standard deviation), while the median (interquartile range (IQR)) was used for non-normal data. Categorical data were described as a number (percentage). The proportion of the categorical variables was compared using a chi-square analysis or Fisher’s exact

test, as appropriate. In the case of non-normally distributed variables, the Mann–Whitney *U* test was used. All statistical analyses were performed using STATA statistical analysis software (version 16).

3 Results

3.1 Study population

Forty patients with *PsAF* were enrolled in this study. Demographic, clinical and instrumental characteristics of the study population are reported in Table 1. Overall, the mean age was 62.2 ± 7.4 years; males were 72.5% ($n = 29$), and the mean CHA₂DS₂-VASC was 2.3 ± 0.9 . The mean left ventricular systolic function was $60.2 \pm 10.3\%$, while LA index volume was 41.0 ± 14.7 ml/m².

Table 1 Baseline characteristics of study population

Study population <i>N</i> =40	
Demographics characteristics	
Age (years)	62.2 ± 7.4
Male sex	29 (72.5)
BMI (kg/m ²)	28.0 ± 4.4
Clinical data	
Hypertension	26 (65)
Dyslipidaemia	11 (27.5)
Diabetes	4 (10)
Smoking	5 (12.5)
Stroke	1 (2.5)
Ischaemic cardiomyopathy	1 (2.5)
Peripheral artery disease	1 (2.5)
COPD	5 (12.5)
CHA ₂ DS ₂ -VASC	2.3 ± 0.9
Persistent AF duration	
< 6 months	4 (10)
6–12 months	21 (52.5)
> 12 months	15 (37.5)
Cardiac function and chamber dimensions	
LVEF (%)	60.2 ± 10.3
LA volume (ml)	80.1 ± 28.0
Indexed LA volume (ml/m ²)	41.0 ± 14.7

Data are presented as mean ± standard deviation or *n.* (%)

AF atrial fibrillation, BMI body mass index, COPD chronic obstructive pulmonary disease, LA left atrium, LVEDD left ventricular end-diastolic diameter, LVEF left ventricular ejection fraction

AF duration was < 6 months in 4 patients (10%), between 6 and 12 months in 21 patients (52.5%) and > 12 months in 15 patients (37.5%).

3.2 AEDUM areas in SR

AEDUM map was obtained in all patients after at least one ECV. The mean number of points used in the 3D LA map was 3053 ± 711 and the heart rate during mapping procedure was 65 ± 7 bpm. The findings obtained from AEDUM maps are summarized in Table 2. The mean overall EGM duration recorded in PsAF was 49.0 ± 16.2 ms, while the maximum duration of EGMs was 90 ± 19 ms. All patients had at least one AEDUM area, and the mean EGM duration was significantly longer in the AEDUM areas than in the remaining LA (58.2 ± 16.9 ms vs 38.3 ± 4.7 ms; *p*-value < 0.001). In PsAF patients, the mean cumulative AEDUM area was 21.8 ± 8.2 cm².

The overall bipolar voltage of the LA was 3.06 ± 1.87 mV. The bipolar voltage of the AEDUM areas was lower than in the remaining atrial areas (median 1.30 mV (IQR 0.71–2.38 mV) vs 1.54 mV (IQR 0.79–2.97 mV); *p*-value < 0.001). LVA was reported in three patients (7.5%)

Table 2 Electroanatomic maps collected during sinus rhythm

Study population <i>N</i> =40	
Number of points used	3053 ± 711
Voltage	
Mean voltage (mV)	3.06 ± 1.87
Patients with areas of low voltage (%)	3 (7.5)
Total area of low voltage (cm ²)	9.1 ± 6.2
AEDUM	
Patients with AEDUM areas	40 (100)
AEDUM area extension (cm ²)	21.8 ± 8.2
AEDUM extension indexed for LA surface (%)	23.4 ± 9.1
Mean maximum duration (ms)	90 ± 19
Overall EGM duration (ms)	49.0 ± 16.2

Data are presented as mean ± standard deviation or *n.* (%)

AEDUM atrial electrogram duration map, LA left atrial

and were identified in one case on the roof toward the right superior pulmonary vein and two cases in the anterior wall. The overall distribution of the AEDUM area is reported in Fig. 2.

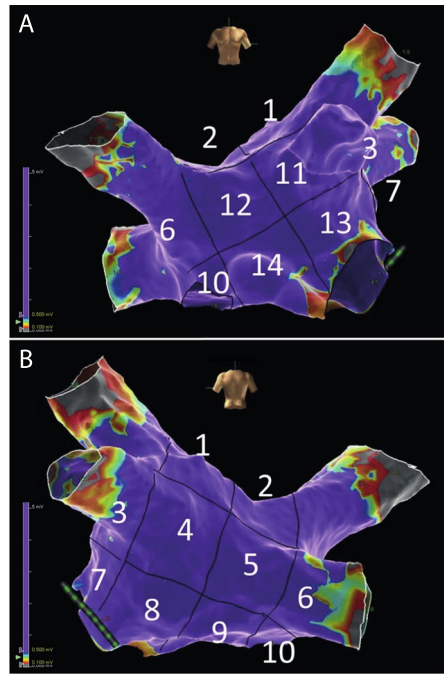
3.3 STED areas in PsAF

The LA maps obtained during AF showed STED areas in all patients (Table 3). A mean of 3458 ± 704 points per patient was used in the analysis. The mean area of dispersed and rapid atrial EGMs (< 60 ms) was 23.9 ± 15.3 cm² which covered 25 ± 15% of the LA surface. The mean number of segments with STED < 60 ms was 6 ± 3 per patient. The overall distribution of the STED area is described in Fig. 2. The mean area of dispersed and rapid atrial EGMs (< 120 ms) was 46.3 ± 20.2 cm² which covered 45 ± 22% of the LA surface.

3.4 Comparison between AEDUM and STED

The overall extension of the AEDUM areas was similar to the STED areas with *CL* < 60 ms (21.8 ± 8.2 vs 23.9 ± 15.3 cm²; *p*-value: 0.37), while it was significantly smaller than STED areas with *CL* < 120 ms (21.8 ± 8.2 vs 46.3 ± 20.2; *p*-value < 0.0001). In 24 patients (60%), AEDUM areas were entirely included in the STED areas with *CL* < 120 ms (Fig. 3). No significance difference was reported in the mean number of LA segments with AEDUM and STED area (7 ± 3 vs 6 ± 3 respectively; *p*-value 0.3). As reported in Fig. 2, AEDUM and STED areas are most frequently reported on the roof, the anterior wall and the septum of the LA. In particular, STED areas were more commonly identified in the posterior (segments 5 and 8) and anterior walls (segments 11, 12 and 14) rather than in the AEDUM areas. In

Fig. 2 Localization of the AEDUM and STED areas. AEDUM, atrial electrogram duration map; STED, spatiotemporal electrogram dispersion



Localization of AEDUM and STED Areas			
Site	AEDUM	STED	p-value
1	28 (70)	29 (72.5)	1
2	30 (75)	30 (75)	1
3	13 (32.5)	9 (22.5)	0.45
4	18 (45)	27 (67.5)	0.07
5	18 (45)	28 (70)	0.04
6	40 (100)	30 (75)	0.001
7	7 (17.5)	8 (20)	1
8	13 (32.5)	26 (65)	0.01
9	23 (57.5)	25 (62.5)	0.82
10	27 (67.5)	31 (77.5)	0.45
11	12 (30)	33 (82.5)	0.001
12	25 (62.5)	34 (85)	0.04
13	3 (7.5)	7 (17.5)	0.31
14	13 (32.5)	32 (80)	0.001

Table 3 Electroanatomic maps collected during atrial fibrillation

Study Population
N = 40

Number of points used	3458 ± 704
STED map	
Area of STED < 60 ms	40
Total area (cm ²) of STED < 60 ms	23.9 ± 15.3
Area of STED indexed for LA surface (%)	25 ± 15
Area of STED < 120 ms	40
Total area (cm ²) of STED < 120 ms	46.3 ± 20.2
Area of STED indexed for LA surface (%)	44 ± 23

Data are presented as mean ± standard deviation or n. (%)

AEDUM atrial electrogram duration map, LA left atrium, STED spatiotemporal electrogram dispersion

the three patients with LVA, no correspondence with STED and AEDUM areas was noted (Fig. 4).

3.5 Clinical follow-up

During the follow-up (median 511 days (376–845 days) 20 (50%) patients experienced clinical recurrence of AF or atrial flutter/tachycardia. Electroanatomical characteristics of the index procedure are reviewed for all patients and are reported in Supplementary Table 1. Electroanatomic maps showed higher maximum duration of EGMs recorded in patients who experienced clinical recurrence than without

(98 ± 19 vs 79 ± 11 ms; p-value 0.02). Otherwise, no difference was reported in terms of extension of AEDUM and STED area and bipolar voltage between groups.

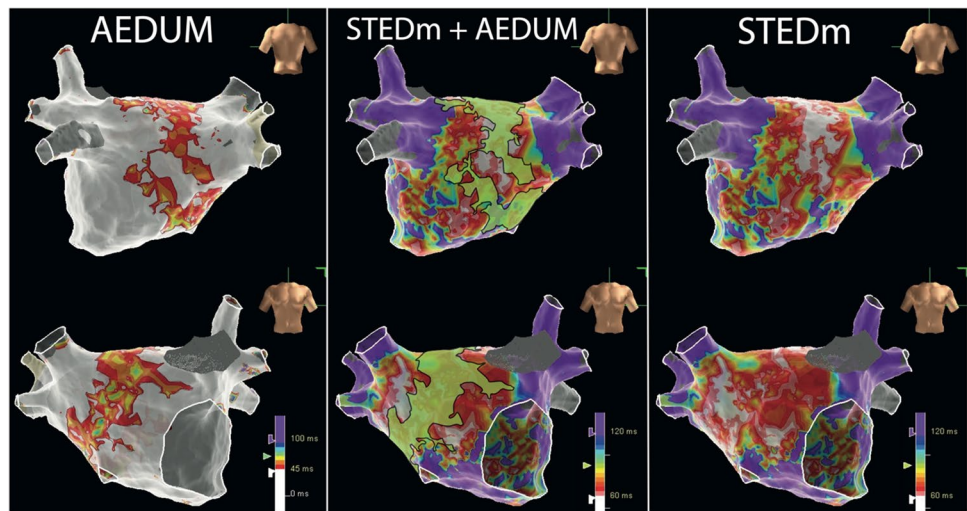
4 Discussion

We report our clinical experience about different mapping functional methods for the identification of local conductive abnormalities necessary for perpetuating *PsAF*.

The main findings of our study are the following:

- All patients had at least one AEDUM area, and they are frequently located on the roof, the anterior wall and the septum of the LA.
- STED areas covered approximately half LA surface (45 ± 22%) and were more commonly identified in the posterior wall than the AEDUM areas. The extension of the AEDUM areas was significantly smaller than STED areas (21.8 ± 8.2 vs 46.3 ± 20.2; p-value < 0.0001). Only in the 60% of cases, AEDUM areas were entirely included in the STED areas.
- LVAs were reported in a small percentage of patients with *PsAF* (7.5%), and no correspondence with STED and AEDUM was recognized.
- Longer EGM durations were found in patients who experienced AF recurrence during follow-up. Otherwise, no difference was reported in terms of extension of AEDUM and STED area and bipolar voltage between groups.

Fig. 3 Comparison between AEDUM and STED areas. Left panels represent posterior and anterior views of AEDUM during SR while and right panels depict posterior and anterior views of STED map during AF. Center panels, the AEDUM areas are superimposed to the STED areas; this figure supports the hypothesis that the AEDUM areas of slow conduction may play an active role in the disorganization of electrical conduction during AF. AEDUM, atrial electrogram duration map; AF, atrial fibrillation; SR, sinus rhythm; STED, spatiotemporal electrogram dispersion



4.1 EGM duration map

Multiple functional approaches have been developed to target local conductive inhomogeneous areas necessary for the maintenance of *PsAF* [12–14, 17, 22]. The pivotal

hypothesis of these methods is that EGM duration and its characteristics are the epiphenomenon of atrial remodeling and augmented non-uniform anisotropism [23, 24]. In *PsAF* patients, atrial tissue remodeling is characterized by patchy and/or interstitial fibrosis, modification of spatial

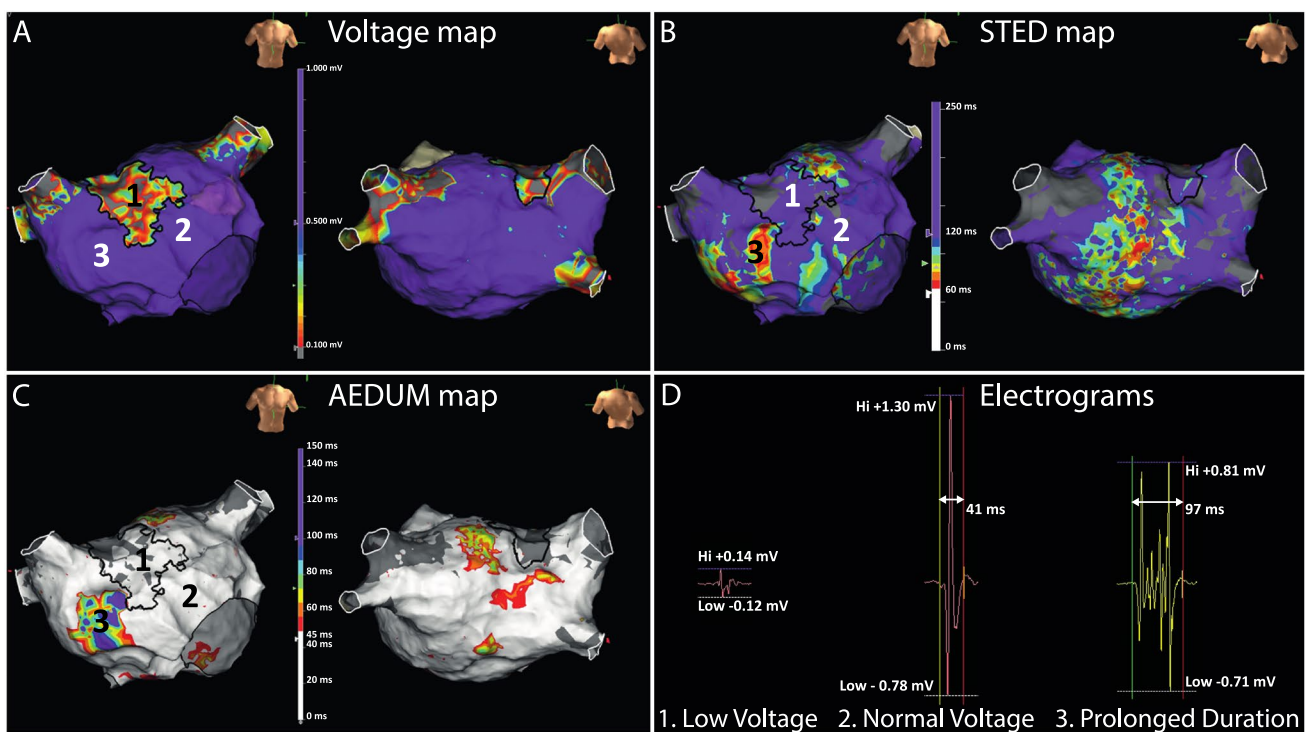


Fig. 4 Comparison of LVA, AEDUM and STED areas. In this figure are reported the maps of the patient with *PsAF* with LVA. Voltage map (panel A), STED map (panel B) and AEDUM map (panel C) are shown. In panel A, the voltage map shows a LVA on the right part of the left atrial roof and anterior wall. The boundaries of the LVA (area 1) are also depicted on the STED map (panel B) and the AEDUM map (panel C); no correlation is reported between LVA and STED and AEDUM areas. The area 2 represents healthy tissue since it has

normal voltage and duration in SR and no STED during AF. Instead, the area 3 despite normal voltage has prolonged EGM in SR and high STED during AF. Panel D reports three EGMs collected from areas of low voltage (area 1), normal voltage (area 2) and AEDUM area (area 3). AEDUM, atrial electrogram duration map; AF, atrial fibrillation; EGM, electrogram; LVA: low-voltage area; *PsAF*, persistent atrial fibrillation; SR, sinus rhythm; STED, spatiotemporal electrogram dispersion

distribution of intercellular connexins, gap junction remodeling and muscular tissue disarray [24]. These pathological modifications affect wave propagation between cardiomyocytes, eventually creating substrate for arrhythmia induction and maintenance.

Voltage mapping during AF has been proposed to identify LVA as evidence of regional tissue disease, but this analysis might be hampered due to some confounding factors such as wave-front collisions, responsible for lowering signals' amplitude [25]. On the other hand, bipolar voltage evaluation during SR allows to avoid the tough interpretation of complex signals recorded during AF [26, 27] even if, as we reported in the present study, patients with PsAF do not commonly showed LVAs [28]. Cellular electrical coupling mismatch may be much more implicated than patchy fibrosis; *in vitro* study demonstrated that significant reduction in electrical coupling may produce similar effects to those of severe fibrosis and can modify the dynamics of wave propagation, from planar to reentrant [29]. Therefore, the ablation strategies aiming at targeting LVA highlighted during AF or SR are not widely applicable in patients with PsAF [9–11, 25].

We recently reported how the evaluation of AEDUM map allows the identification of discrete areas of local slow and non-homogeneous conduction suggesting the presence of augmented non-uniform anisotropism. The

utilization of multipolar mapping catheter (HD Grid) permits the recording of EGMs simultaneously from multiple bipoles with different wavefront propagations reducing the underestimation of duration and far-field signal components (Fig. 5). Rapid and fragmented signal registered during AEDUM mapping can be explained by anisotropic conduction, (“zig-zag” conduction) among small muscle bundles. Anisotropic reentries are characterized by marked heterogeneity in conduction velocity, depending on whether the wavefront is propagating in the longitudinal or transverse direction. However slow components could be due to conduction along large muscle bundles, septimented by fibrous strands, with frequent and abrupt changes to their orientation. Moreover, split signals like double potentials were also recorded, representing a block line due to electrical influences during propagation on either side (Fig. 6) [30]. Although the AEDUM study was limited by the small number of patients enrolled, this ablation approach targeting the AEDUM areas resulted in a more effective strategy to treat patients with PsAF.

4.2 Comparison of AEDUM and STED maps

AEDUM areas were largely contained within the boundaries of STED areas (<120 ms) (93% of their total area in 60% of the study group), while in the patients with LVA, no

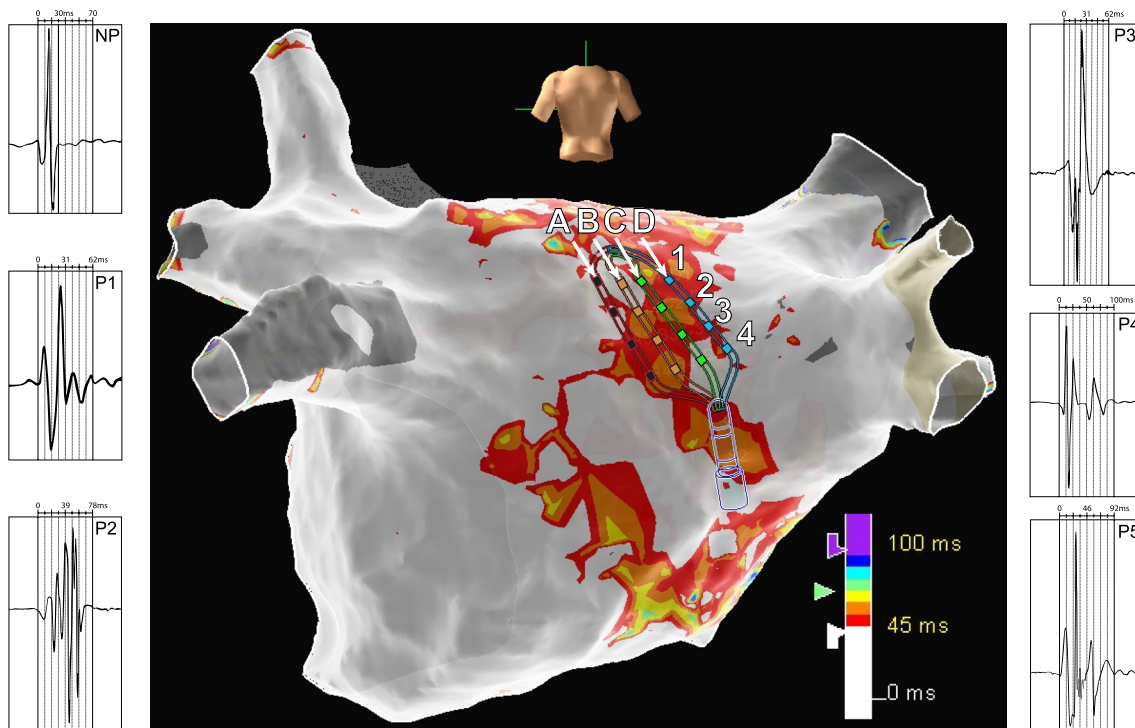


Fig. 5 AEDUM map. The Advisor™ HD Grid Mapping Catheter is positioned on the LA posterior wall registering different dipoles EGM which are annotated in the AEDUM map. While the dipole

A1–A2 records a normal EGM (NP), the potentials P1–5 are recorded from bipoles exploring areas of slow conduction. AEDUM, atrial electrogram duration map; EGM, electrogram; LA, left atrium

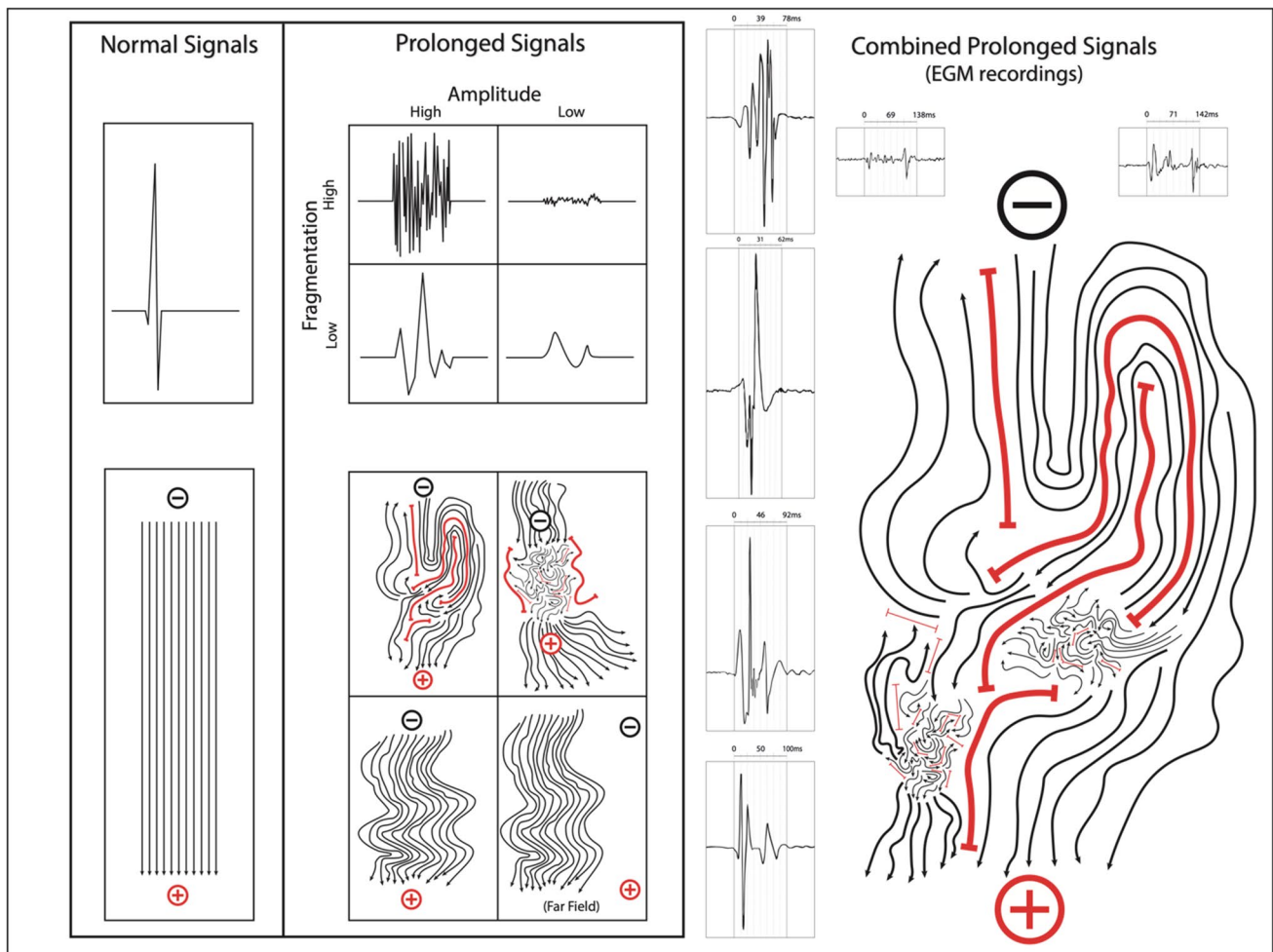


Fig. 6 The genesis of prolonged signals. In the left panel, normal myocardium with “normal signals” conducts wavefronts rapidly with synchronous activation of a large number of cells resulting in sharp EGM with short duration. In the central panel, diseased myocardium with a different degree of fiber disarray and tissue functional remodeling produces disordered propagation, resulting in EGM with prolonged duration and combined slow and rapid signal components.

correspondence with STED and AEDUM was noted. These findings are consistent with published animal data demonstrating that atrial fractionated EGM during AF was co-localized in the regions with more fragmented and longer signals during slow atrial pacing [24]. In our study, the resulting cumulative STED areas were larger if compared with AEDUM areas even though the number of LA segments involved was comparable (7 ± 3 vs 6 ± 3 respectively; p -value 0.3). Surprisingly, if AEDUM and STED areas were either most frequently reported on the roof, the anterior wall and the septum, STED areas were more commonly identified in the posterior wall (Fig. 2). Based on this evidence, we hypothesize the presence of a passively activated area with low rate of tissue fibrosis not

When the process of fibrous septimentation is established, the amplitude of the signals is low. On the contrary, when a process of decoupling of intercellular electrical propagation is prevalent, the voltage can be normal despite a prolonged EGM. As shown in the right panel, during mapping the observed EGM patterns are the result of the multiple combination of the described phenomena. EGM: electrogram

identified during SR that exhibits complex atrial signals mainly due to functional phenomena [31]. Indeed, previous studies have shown that different functional phenomena, like wavefront collision, functional conduction block, wave break and wave fusion, contribute to the genesis of CFAEs [32]. Moreover, in our *PsAF* population, electroanatomic maps showed higher maximum duration of EGMs recorded in patients who experienced clinical recurrence than without recurrence. Otherwise, no difference was reported in terms of extension of AEDUM and STED area and bipolar voltage. The maximum EGM duration as well as other parameters like atrial dimension and p-wave morphology could represent a potential indicator of high risk AF recurrence after catheter ablation [33].

4.3 Limitations

This clinical study has some limitations that should be taken under consideration. Firstly, the size of the study population is restricted and therefore this paper should be considered a pilot study. Larger prospective studies are warranted to confirm our results thus creating solid evidence in identifying patients who will benefit from ablation additional to PVI, eventually targeting AEDUM areas.

Secondly, EGM duration is a functional phenomenon, and the AEDUM area could be influenced by heart rate, site of stimulation or atrial extra stimuli. Another potential limitation is the absence of an automated tool to evaluate bipoles with longer EGM duration. Improved software is needed to automatize the creation of AEDUM maps as much as possible making them more reproducible and thus utilizable in larger cohorts. Additionally, we do not have magnetic resonance imaging data available for the patients included in this study in order to compare EGM and imaging findings. Lastly, we did not verify the effects of anti-arrhythmic or adrenergic/anticholinergic drugs such as isoprenaline/atropine on the AEDUM map.

5 Conclusions

This study demonstrates that the evaluation of AEDUM map can identify areas of conductive dysfunction as a possible atrial substrate even if a normal voltage is detected in patients with *PsAF*. A correspondence between the location of AEDUM areas during SR and STED areas during AF was noted, supporting the hypothesis that local tissue disease underlies the complex and dispersed EGMs during AF.

Supplementary Information The online version contains supplementary material available at <https://doi.org/10.1007/s10840-024-01819-6>.

Data availability The data underlying this article will be shared on reasonable request to the corresponding author.

Declarations

Ethics approval The study protocol was approved by the local ethics committee.

Informed consent Written informed consent from all the patients was obtained before each procedure.

Conflict of interest MN and ADG are currently Abbott employees. All the other authors have nothing to disclose.

References

1. Hindricks G, Potpara T, Dagres N, Arbelo E, Bax JJ, Blomström-Lundqvist C, ... Zakirov NU. 2020 ESC guidelines for

the diagnosis and management of atrial fibrillation developed in collaboration with the European Association for Cardio-Thoracic Surgery (EACTS). *Eur Heart J*. 2021;42(5):373–498. <https://doi.org/10.1093/eurheartj/ehaa612>.

2. Kirchhof P, Calkins H. Catheter ablation in patients with persistent atrial fibrillation. *Eur Heart J*. 2017;38(1):20–6. <https://doi.org/10.1093/eurheartj/ehw260>.
3. Brooks S, Metzner A, Wohlmuth P, Lin T, Wissner E, Tiltz R, ... Ouyang F. Insights into ablation of persistent atrial fibrillation: lessons from 6-year clinical outcomes. *J Cardiovasc Electrophysiol*. 2018;29(2):257–263. <https://doi.org/10.1111/jce.13401>.
4. Nattel S. Molecular and cellular mechanisms of atrial fibrosis in atrial fibrillation. *JACC: Clin Electrophysiol*. 2017;3(5):425–435. <https://doi.org/10.1016/j.jacep.2017.03.002>.
5. Kirubakaran S, Chowdhury RA, Hall MCS, Patel PM, Garratt CJ, Peters NS. Fractionation of electrograms is caused by colocalized conduction block and connexin disorganization in the absence of fibrosis as AF becomes persistent in the goat model. *Heart Rhythm*. 2015;12(2):397–408. <https://doi.org/10.1016/j.hrthm.2014.10.027>.
6. Yamabe H, Morihisa K, Tanaka Y, Uemura T, Enomoto K, Kawano H, Ogawa H. Mechanisms of the maintenance of atrial fibrillation: role of the complex fractionated atrial electrogram assessed by noncontact mapping. *Heart Rhythm*. 2009;6(8):1120–8. <https://doi.org/10.1016/j.hrthm.2009.04.021>.
7. Kalifa J, Tanaka K, Zaitsev AV, Warren M, Vaidyanathan R, Auerbach D, ... Berenfeld O. Mechanisms of wave fractionation at boundaries of high-frequency excitation in the posterior left atrium of the isolated sheep heart during atrial fibrillation. *Circulation*. 2006;113(5):626–633. <https://doi.org/10.1161/CIRCULATIONAHA.105.575340>.
8. Frontera A, Pagani S, Limite LR, Peirone A, Fioravanti F, Enache B, ... Della Bella P. Slow conduction corridors and pivot sites characterize the electrical remodeling in atrial fibrillation. *JACC: Clin Electrophysiol*. 2022;8(5):561–577. <https://doi.org/10.1016/j.jacep.2022.01.019>.
9. Jadidi AS, Lehrmann H, Keyl C, Sorrel J, Markstein V, Minners J, ... Arentz T. Ablation of persistent atrial fibrillation targeting low-voltage areas with selective activation characteristics. *Circ Arrhythmia Electrophysiol*. 2016;9(3):e002962. <https://doi.org/10.1161/CIRCEP.115.002962>.
10. Kottkamp H, Schreiber D, Moser F, Rieger A. Therapeutic approaches to atrial fibrillation ablation targeting atrial fibrosis. *JACC: Clin Electrophysiol*. 2017;3(7):643–653. <https://doi.org/10.1016/j.jacep.2017.05.009>.
11. Yagishita A, Gimbel JR, De Oliveira S, Manyam H, Sparano D, Cakulev I, ... Arruda M. Long-term outcome of left atrial voltage-guided substrate ablation during atrial fibrillation: a novel adjunctive ablation strategy. *J Cardiovasc Electrophysiol*. 2017;28(2):147–155. <https://doi.org/10.1111/jce.13122>.
12. Nademanee K, McKenzie J, Kosar E, Schwab M, Sunsaneewitayakul B, Vasavakul T, ... Ngarmukos T. A new approach for catheter ablation of atrial fibrillation: mapping of the electrophysiologic substrate. *J Am Coll Cardiol*. 2004;43(11):2044–2053. <https://doi.org/10.1016/j.jacc.2003.12.054>.
13. Lațcu DG, Enache B, Hasni K, Wedn AM, Zaqane N, Pathak A, Saoudi N. Sequential ultrahigh-density contact mapping of persistent atrial fibrillation: an efficient technique for driver identification. *J Cardiovasc Electrophysiol*. 2021;32(1):29–40. <https://doi.org/10.1111/jce.14803>.
14. Seitz J, Bars C, Théodore G, Beurtheret S, Lellouche N, Bremond M, ... Kalifa J. AF ablation guided by spatiotemporal electrogram dispersion without pulmonary vein isolation. *J Am Coll Cardiol*. 2017;69(3):303–321. <https://doi.org/10.1016/j.jacc.2016.10.065>.
15. Sau A, Kapadia S, Al-Aidarous S, Howard J, Sohaib A, Sikkell MB, ... Ng FS. Temporal trends and lesion sets for persistent

- atrial fibrillation ablation: a meta-analysis with trial sequential analysis and meta-regression. *Circ Arrhythmia Electrophysiol.* 2023;16(9). <https://doi.org/10.1161/CIRCEP.123.011861>.
16. Wu S, Li H, Yi S, Yao J, Chen X. Comparing the efficacy of catheter ablation strategies for persistent atrial fibrillation: a Bayesian analysis of randomized controlled trials. *J Interv Card Electrophysiol.* 2022. <https://doi.org/10.1007/s10840-022-01246-5>.
 17. Rossi P, Cauti FM, Polselli M, Magnocavallo M, Niscola M, Fanti V, ... Bianchi S. Ablation of persistent atrial fibrillation based on atrial electrogram duration map: methodology and clinical outcomes from the AEDUM pilot study. *J Interv Cardiac Electrophysiol.* 2024. <https://doi.org/10.1007/s10840-023-01721-7>.
 18. Rodríguez-Mañero M, Valderrábano M, Baluja A, Kreidieh O, Martínez-Sande JL, García-Seara J, ... Sarkozy A (2018). Validating left atrial low voltage areas during atrial fibrillation and atrial flutter using multielectrode automated electroanatomic mapping. *JACC: Clin Electrophysiol.* 2018;4(12):1541–1552. <https://doi.org/10.1016/j.jacep.2018.08.015>.
 19. Rossi P, Cauti FM, Niscola M, Magnocavallo M, Polselli M, Capone S, ... Bianchi S. Ventricular electrograms duration map to detect ventricular arrhythmia substrate: the vedum project study. *Circ Arrhythmia Electrophysiol.* 2023;16(8):447–455. <https://doi.org/10.1161/CIRCEP.122.011729>.
 20. Hunter RJ, Diab I, Tayebjee M, Richmond L, Sporton S, Earley MJ, Schilling RJ. Characterization of fractionated atrial electrograms critical for maintenance of atrial fibrillation: a randomized, controlled trial of ablation strategies (the CFAE AF trial). *Circ Arrhythmia Electrophysiol.* 2011;4(5):622–9. <https://doi.org/10.1161/CIRCEP.111.962928>.
 21. Rossi P, Cauti FM, Limite LR, Iaia L, Allegretti G, Di Renzi P, ... Bianchi S. Interatrial conduction times in paroxysmal atrial fibrillation patients with normal atrial volume and their correlation with areas of local prolonged bipolar electrograms. *J Electrocardiol.* 2020;58:19–26. <https://doi.org/10.1016/j.jelecard.2019.09.017>.
 22. Rossi P, Cauti FM, Polselli M, Bianchi S. Map of prolonged electrogram duration to guide atrial substrate ablation for atrial fibrillation recurrence following durable pulmonary vein isolation. *J Innov Cardiac Rhythm Manag.* 2020;12(S1):35–36. <https://doi.org/10.19102/icrm.2021.120124S>.
 23. Verma A, Jiang C, Betts TR, Chen J, Deisenhofer I, Mantovan R, ... Sanders P. Approaches to catheter ablation for persistent atrial fibrillation. *N Engl J Med.* 2015;372(19):1812–1822. <https://doi.org/10.1056/NEJMoa1408288>.
 24. Campos FO, Wiener T, Prassl AJ, Weber dos Santos R, Sanchez-Quintana D, Ahammer H, ... Hofer E. Electroanatomical characterization of atrial microfibrosis in a histologically detailed computer model. *IEEE Trans Biomed Eng.* 2013;60(8):2339–2349. <https://doi.org/10.1109/TBME.2013.2256359>.
 25. Qureshi NA, Kim SJ, Cantwell CD, Afonso VX, Bai W, Ali RL, ... Lim PB. Voltage during atrial fibrillation is superior to voltage during sinus rhythm in localizing areas of delayed enhancement on magnetic resonance imaging: an assessment of the posterior left atrium in patients with persistent atrial fibrillation. *Heart Rhythm.* 2019;16(9):1357–1367. <https://doi.org/10.1016/j.hrthm.2019.05.032>.
 26. Blandino A, Bianchi F, Grossi S, Biondi-Zoccai G, Conte MR, Gaido L, ... Rametta F. Left atrial substrate modification targeting low-voltage areas for catheter ablation of atrial fibrillation: a systematic review and meta-analysis: low-voltage af ablation meta-analysis. *Pacing Clin Electrophysiol.* 2017;40(2):199–212. <https://doi.org/10.1111/pace.13015>.
 27. Sim I, Bishop M, O'Neill M, Williams SE. Left atrial voltage mapping: defining and targeting the atrial fibrillation substrate. *J Interv Card Electrophysiol.* 2019;56(3):213–27. <https://doi.org/10.1007/s10840-019-00537-8>.
 28. Rossi P, Cauti FM, Polselli M, Corradetti S, Bianchi S. Local inhomogeneous conduction and non-uniform anisotropism in a normal voltage atrial map. *J Interv Card Electrophysiol.* 2022;64(3):759–60. <https://doi.org/10.1007/s10840-022-01162-8>.
 29. Bub G, Shrier A, Glass L. Spiral wave generation in heterogeneous excitable media. *Phys Rev Lett.* 2002;88(5):058101. <https://doi.org/10.1103/PhysRevLett.88.058101>.
 30. Schalij MJ, Boersma L, Huijberts M, Allessie MA. Anisotropic reentry in a perfused 2-dimensional layer of rabbit ventricular myocardium. *Circulation.* 2000;102(21):2650–8. <https://doi.org/10.1161/01.CIR.102.21.2650>.
 31. Rostock T, Rotter M, Sanders P, Takahashi Y, Jaïs P, Hocini M, ... Haïssaguerre M. High-density activation mapping of fractionated electrograms in the atria of patients with paroxysmal atrial fibrillation. *Heart Rhythm.* 2006;3(1):27–34. <https://doi.org/10.1016/j.hrthm.2005.09.019>.
 32. Gerstenfeld EP, Lavi N, Bazan V, Gojraty S, Kim SJ, Michele J. Mechanism of complex fractionated electrograms recorded during atrial fibrillation in a canine model. *Pacing Clin Electrophysiol.* 2011;34(7):844–57. <https://doi.org/10.1111/j.1540-8159.2011.03071.x>.
 33. Knecht S, Pradella M, Reichlin T, Mühl A, Bossard M, Stieltjes B, ... Sticherling C. Left atrial anatomy, atrial fibrillation burden, and P-wave duration—relationships and predictors for single-procedure success after pulmonary vein isolation. *EP Europace.* 2018;20(2):271–278. <https://doi.org/10.1093/europace/euw376>

Publisher's Note Springer Nature remains neutral with regard to jurisdictional claims in published maps and institutional affiliations.

Springer Nature or its licensor (e.g. a society or other partner) holds exclusive rights to this article under a publishing agreement with the author(s) or other rightsholder(s); author self-archiving of the accepted manuscript version of this article is solely governed by the terms of such publishing agreement and applicable law.